Cancer Biol Med 2024. doi: 10.20892/j.issn.2095-3941.2023.0248

ORIGINAL ARTICLE

Cancer-educated neutrophils promote lung cancer progression *via* PARP-1-ALOX5-mediated MMP-9 expression

Lulu Han[1,2,3], Yuxin Chen[1,2,3], Nan Huang[1], Xiaowan Zhou[1,4], Yanfang Lv[1], Huizhong Li[1,2,3], Dafei Chai[1,2,3], Junnian Zheng[2,3], Gang Wang[1,2,3]

[1]Cancer Institute, Xuzhou Medical University, 209 Tongshan Road, Xuzhou 221004, China; [2]Center of Clinical Oncology, The Affiliated Hospital of Xuzhou Medical University, 99 West Huaihai Road, Xuzhou 221002, China; [3]Jiangsu Center for the Collaboration and Innovation of Cancer Biotherapy, Xuzhou Medical University, 209 Tongshan Road, Xuzhou 221004, China; [4]Department of Oncology, Suzhou Xiangcheng People's Hospital, Suzhou 215131, China

ABSTRACT

Objective: Neutrophils are one of the most predominant infiltrating leukocytes in lung cancer tissues and are associated with lung cancer progression. How neutrophils promote lung cancer progression, however, has not been established.

Methods: Kaplan–Meier plotter online analysis and tissue immunohistochemistry were used to determine the relationship between neutrophils and overall survival in lung cancer patients. The effect of neutrophils on lung cancer was determined using the Transwell migration assay, a proliferation assay, and a murine tumor model. Gene knockdown was used to determine poly ADP-ribose polymerase (PARP)-1 function in lung cancer-educated neutrophils. Western blot analysis and gelatin zymography were used to demonstrate the correlation between PARP-1 and matrix metallopeptidase 9 (MMP-9). Immunoprecipitation coupled to mass spectrometry (IP/MS) was used to identify the proteins interacting with PARP-1. Co-immunoprecipitation (Co-IP) was used to confirm that PARP-1 interacts with arachidonate 5-lipooxygenase (ALOX5). Neutrophil PARP-1 blockage by AG14361 rescued neutrophil-promoted lung cancer progression.

Results: An increased number of infiltrating neutrophils was negatively associated with overall survival in lung cancer patients ($P < 0.001$). Neutrophil activation promoted lung cancer cell invasion, migration, and proliferation *in vitro*, and murine lung cancer growth *in vivo*. Mechanistically, PARP-1 was shown to be involved in lung cancer cell-induced neutrophil activation to increase MMP-9 expression through interacting and stabilizing ALOX5 by post-translational protein modification (PARylation). Blocking PARP-1 by gene knockdown or AG14361 significantly decreased ALOX5 expression and MMP-9 production, and eliminated neutrophil-mediated lung cancer cell invasion and *in vivo* tumor growth.

Conclusion: We identified a novel mechanism by which PARP-1 mediates lung cancer cell-induced neutrophil activation and PARylates ALOX5 to regulate MMP-9 expression, which exacerbates lung cancer progression.

KEYWORDS Lung cancer; neutrophils; PARP-1; ALOX5; MMP-9

Introduction

Worldwide, lung cancer remains the leading cause of cancer deaths, with an estimated 1.8 million deaths each year[1,2]. Neutrophils have been identified as the dominant immune cells in the human lung cancer microenvironment[3]. Increased neutrophil infiltration is strongly associated with lung cancer recurrence[4]. Additionally, studies have demonstrated that an increased absolute peripheral blood neutrophil count and neutrophil-to-lymphocyte ratio are negatively correlated with prognosis in lung cancer patients[5-7] and the clinical efficacy of immune checkpoint inhibitors[8]. Multifaceted roles of neutrophils have been reported in cancer progression[9,10]. During the initial stage of cancer, neutrophils have an anti-tumor function by activating the T cell response[11], then neutrophils have a tumor-promoting phenotype after exposure to the tumor microenvironment[12,13]. A recent study demonstrated that neutrophils reprogrammed by lung mesenchymal cells promote cancer metastasis[14]. After education and activation, tumor-infiltrating neutrophils

Correspondence to: Junnian Zheng and Gang Wang
E-mail: jnzheng@xzhmu.edu.cn and wangg@xzhmu.edu.cn
ORCID ID: https://orcid.org/0000-0003-0208-6410
and https://orcid.org/0000-0001-6020-7263
Received August 8, 2023; accepted December 6, 2023;
published online January 2, 2024.
Available at www.cancerbiomed.org

release a large number of cytokines and proteases, such as interleukin (IL)-8, IL-17, matrix metallopeptidase 9 (MMP-9), vascular endothelial growth factor (VEGF), elastase, and arginase[15], which promote inflammatory cell infiltration, tumor angiogenesis, tumor metastasis, and immune escape[9]. Depletion of neutrophils by neutralizing antibodies has shown promising therapeutic effects in multiple murine tumor models[16]; however, human neutrophil depletion is unattainable in cancer patients because of the significant risk of infection. Therefore, a better understanding of the molecular mechanism underlying tumor-educated neutrophil activation will help identify new therapeutic targets for cancer therapy.

Poly ADP-ribose polymerase-1 (PARP-1) is a DNA repair enzyme that is critical in regulating DNA damage repair[17] and post-translational protein modification (PARylation) by transferring ADP-ribose units onto protein substrates[18]. PARP-1 was the first PARP family molecule to be identified. An increasing number of reports have shown that PARP-1 has a crucial role in regulating and maintaining tissue inflammation[19]. Our previous study showed that blocking PARP-1 inhibits the recruitment and activation of neutrophils by inhibiting the nuclear factor kappa-light-chain-enhancer of activated B cells (NF-κB) pathway in lipopolysaccharide (LPS)-induced acute lung inflammation[20]. Moreover, PARP-1 inhibition significantly reduces neutrophilic inflammation in mouse lungs[21]. Neutrophil activation and retention in tumor cells also aggravates tissue damage, suppresses immune responses, and promotes tumor progression[22]. PARP-1 inhibition enhances anti-tumor immunity in mouse models and lung cancer patients[23]. Accordingly, we reasoned that PARP-1 may regulate neutrophil activation and thus affect lung cancer progression.

In this study we showed that neutrophil infiltration increased in lung cancer tissues and was negatively correlated with patient prognosis. Our study identified neutrophil-released MMP-9 as a powerful pro-lung cancer protein. Additionally, increasing PARP-1 in neutrophils educated by lung cancer cells interacted with arachidonate 5-lipoxygenase (ALOX5) and promoted stabilization of ALOX5 *via* PARylation to mediate neutrophil activation and MMP-9 expression. Furthermore, we demonstrated that blocking neutrophil PARP-1 inhibited lung cancer progression in mice. This study provides a novel intervention target and therapeutic strategy for neutrophil hyperactivity in lung cancer progression.

Materials and methods

Patients and samples

Tissue microarray containing cancer and para-cancer tissues from 75 patients with stage I–III lung adenocarcinoma and clinical pathologic information was purchased from Shanghai Outdo Biotech (Approval No. YBM-05-01; Shanghai, China). The Ethics Committee of Xuzhou Medical University approved the use of the microarray for immunohistochemistry (IHC) staining.

IHC staining

IHC was performed using the streptavidin-peroxidase (SP) technique with a standard SP Kit (PV-9000; ZSGB-BIO, Beijing, China) for myeloperoxidase (MPO) staining. Briefly, a tissue microarray slide was incubated with monoclonal rabbit anti-MPO antibody (1:250 dilution, ab134132; Abcam, Cambridge, MA, USA) overnight at 4°C after dewaxing, antigen retrieval, and blocking. Then, HRP-conjugated goat anti-rabbit IgG antibody (ZSGB-BIO, Beijing, China) was incubated at room temperature for 2 h before precipitation with diaminobenzidine [DAB] (ZLI-9018; ZSGB-BIO, Beijing, China). MPO-positive cells with polymorphic nuclei were counted under light microscopy and recorded in each tissue to quantify tissue-infiltrating neutrophils.

Subcutaneous graft tumor tissues from mice with the indicated treatments described below were fixed in 4% paraformaldehyde for 12 h for Ki67 staining. Next, tumor tissues were paraffin-embedded and sectioned at a thickness of 5 μm. Then, the sections were stained with anti-Ki67 (#GB111499; ServiceBio, Wuhan, China). Ki67 staining and analysis were performed according to the protocol described in our previous paper[24].

Cell culture and transfection

HL-60 cells were purchased from the American Type Culture Collection [ATCC] (Manassas, VA, USA) and maintained in RPMI-1640 complete medium containing 10% fetal bovine serum [FBS] (Hyclone, Logan, Utah, USA) and 1% penicillin-streptomycin [PS] (ST488; Beyotime, Shanghai, China). HL-60 cells were differentiated with the addition of 1.3% dimethyl sulfoxide [DMSO] (D2550; Sigma, St. Louis, MO, USA) into

the medium for 5–7 days to obtain neutrophil-like cells, according to the method detailed in our previous report[25]. Lewis lung carcinoma (LLC) cells were purchased from Procell Life Science & Technology (CL-0140; Wuhan, China) and cultured in Dulbecco's modified Eagle Medium (DMEM) complete medium containing 10% FBS and 1% PS. Human lung adenocarcinoma cell lines (A549 and H1299) were purchased from ATCC and cultured in DMEM and RPMI-1640 complete medium, respectively. The cell lines mentioned above were cultured in a 5% (v/v) CO_2 humidified incubator at 37°C.

Bone marrow neutrophils (BMNs) isolated from wild-type C57BL/6 (C57) mice (Xuzhou Medical University, Xuzhou, China) were purified by gradient centrifugation according to the protocol described in our previous papers[25,26].

Control short hairpin (sh)RNA or PARP-1 shRNA plasmids were purchased from Santa Cruz Biotechnology, Inc. (Santa Cruz, CA, USA) and co-transfected with the helper plasmids, pMD2.G and psPAX2, into 293T cells to produce pseudoviral particles. The supernatant containing pseudoviral particles was collected after 48 h and used to infect HL-60 cells to interfere with PARP-1 expression. The PARP-1 knock-down (PARP-1^{kd}) effect was detected by western blot after three consecutive days of puromycin screening.

pCMV3-Flag-PARP-1 (Sino Biological, Beijing, China) and pCMV3-HA-ALOX5 plasmids (Miaoling Biology, Wuhan, China) were co-transfected into 293T cells in 6-well plates with 2 μg plasmids per well using Lipofectamine 2000 (Invitrogen, Carlsbad, CA, USA). The cells were lysed with buffer for immunoprecipitation with anti-Flag (F1804; Sigma) and anti-HA antibody (Santa Cruz Biotechnology, Inc.) after 48 h.

Preparation of neutrophil activation supernatant

Neutrophils (1×10^7 cells/mL) that were differentiated from HL-60 cells as described above or BMNs from mice were stimulated by adding 1 μg/mL of LPS for 4 h in a 5% (v/v) CO_2 humidified incubator at 37°C to obtain a neutrophil-activated population. For ALOX5 inhibition or the control group, 50 mM Zileuton (S1443; Selleckchem, Houston, TX, USA), an ALOX5 inhibitor, or 0.1% DMSO was used to create the activated production. The supernatants were defined as activated production and the activated neutrophils were collected for a gelatin zymography assay, an invasion and migration assay, reverse transcription polymerase chain reaction (RT-PCR), a proliferation assay, and western blot analysis.

Co-culture assay (tumor cell-educated neutrophils)

To collect the supernatants and neutrophils for further studies, A549, H1299, or LLC cells were seeded into 6-well plates. Neutrophils from HL-60 cell differentiation or BMNs (1×10^7 cells in 1 mL of RPMI-1640 without FBS) were suspended and added to the plates when cancer cells had grown to approximately 90% confluence, which was defined as the co-culture. Then, the supernatants and neutrophils were collected immediately after 4 h for subsequent assay.

Invasion and migration assay

The activated production was obtained for this experiment as described above. The upper chambers of a Transwell system (8-μm pore size, 15215031; Costar, Kennebunk, ME, USA) were pre-coated with growth factor-reduced Matrigel (serum-free DMEM = 1:9, 356234; BD Biosciences, Franklin Lakes, NJ, USA) for 5 h prior to use in the invasion assay. A549, H1299, or LLC cells were plated in the upper chamber at a density of 5×10^4 cells per well in 50 μL of serum-free medium with 50 μL of neutrophil activation supernatant and 5% or 1% FBS supplemented medium in the lower chamber as a chemoattractant. For the target signaling inhibition assay, 50 mM Zileuton or 200 μM 1.10 phenanthroline [1,10PE] (131377; Sigma), an inhibitor of zinc-dependent MMP-9, was added to the chambers, which were incubated under standard tissue culture conditions for 12 h. After incubation, the cells in the upper chambers were removed. The cells that had passed through the membrane were fixed in methanol, stained with crystal violet, then counted. The number of invaded cells was averaged in five random fields. The cells were plated in the upper chamber without Matrigel in the migration assay. Neutrophils (6×10^6 in 600 μL of serum-free medium) were pre-seeded in the lower chamber for co-culture studies.

Cell proliferation assay

Cell proliferation was detected using the Cell Counting Kit-8 (CCK8) assay kit (Vicmed, Nanjing, China). Briefly, A549 or H1299 cells were seeded into 96-well plates and treated with neutrophil-activated production with or without the inhibitors indicated above for different times (0, 24, 48, and 72 h). Then, 10 μL of CCK8 solution with 90 μL of serum-free medium was added to each well and the plates were incubated

at 37°C for another 1–2 h. Absorbance at 450 nm was measured with a BioTek Cytation 3 imaging reader (Beijing, China).

Quantitative real-time PCR assay

The HL-60 cells were differentiated with DMSO and co-cultured with A549 or H1299, as described above. BMNs were co-cultured with LLC cells, as described above. Then, the total RNA of the cells was extracted with TRIzol Reagent (Life Technologies, Grand Island, NY, USA) following the manufacturer's instructions, and cDNA synthesis was performed with a HiScript® RT-PCR Kit (R123-01; Vazyme Biotech, Nanjing, China). Real-time PCR amplification of *ccl5*, *ccl2*, *mmp-9*, *arg-1*, *cxcr4*, and *vegf* mRNA (Bgitech, Shenzhen, China) was performed for 10 min at 95°C, followed by 40 cycles at 95°C for 10 s, and annealing at 60°C for 34 s using an ABI PRISM 7500 Sequence Detection System (Grand Island, NY, USA), with β-actin as an internal control. The primer sequences are listed in **Table S1**.

Gelatin zymography assay

Neutrophils were treated with LPS, as described above. Four hours after activation, the supernatants were harvested at 4°C and mixed with a non-reducing sample buffer. Then, the samples were separated by 10% SDS-PAGE electrophoresis containing 0.1% gelatin. After electrophoresis, the gel was washed with washing buffer (2.5% Triton X-100 in a reaction buffer), then incubated in reaction buffer [50 mM Tris–HCl, 5 mM $CaCL_2$, and 1 μM $ZnCl_2$ (pH 7.4)] for 36 h at 37°C. The gel was stained with Coomassie brilliant blue R-250 for 4 h and destained in 50% methanol, 40% distilled water, and 10% acetic acid to visualize the bands. Gelatinolytic activity was shown as clear areas in the gel. Gels were photographed, then analyzed quantitatively.

Western blot analysis

The cells, which were treated as described above, were washed twice in PBS and immediately lysed with RIPA buffer containing 1% protease inhibitor (P8340; Sigma). Protein concentrations in the cell lysate solutions were determined using the BCA protein assay (Amresco, Cochran, GA, USA). Each cell lysate was mixed with 2 × SDS-PAGE loading buffer (Bio-Rad, Waltham, MA, USA). Equivalent protein quantities were loaded onto 12% SDS-polyacrylamide gels (Bio-Rad). Proteins were electro-transferred to nitrocellulose (NC) membranes (PALL Corporation, Mexico City, Mexico) that were blocked in Tris-buffered saline plus 0.05% Tween-20 (TBS-T) containing 5% non-fat dried milk for 1 h. The membranes were washed in TBS-T and incubated with each primary monoclonal antibody overnight at 4°C. The following primary antibodies were used: rabbit anti-PARP-1 (sc-1561; Santa Cruz Biotechnology, Inc.); and anti-MMP-9, anti-ALOX5, anti-GAPDH, and anti-actin monoclonal antibody (1:1000 dilution; Cell Signaling Technology, Danvers, MA, USA). The immuno-positive bands were visualized with an ECL chemiluminescent detection system (Thermo Scientific, Waltham, MA, USA), and the images were transferred to a Tanon imaging system (Shanghai, China). Densitometry was performed using Image J Software (Bethesda, MD, USA).

Immunoprecipitation coupled to mass spectrometry (IP/MS)

Neutrophils were stimulated with LPS for 4 h at 37°C. Neutrophils were co-cultured with or without A549 or LLC cells, as described above. Then, the neutrophils were washed twice in PBS and solubilized at the indicated time points in RIPA lysis buffer with a complete protease inhibitor cocktail. The lysis debris was cleared after centrifugation at 12,000 × *g* for 10 min. The lysates were then immunoprecipitated with an anti-PARP-1 antibody or an equal amount of normal IgG. Protein A/G Sepharose beads (Santa Cruz Biotechnology, Inc.) were added. After incubation for 2 h at 4°C, the protein A/G Sepharose beads were centrifuged and washed five times with RIPA lysis buffer. The immunoprecipitants were analyzed by immunoblotting. Antibodies for immunoblotting analysis included anti-ALOX5 and anti-PARP-1 antibodies. For PARylation detection, the immunoprecipitants of anti-ALOX5 antibody were analyzed using an anti-PAR antibody (Enzo Life Sciences, Farmingdale, NY, USA) by western blot. For IP/MS, the immunoprecipitants were analyzed by MS (LTQ Orbitrap Velos; Thermo Scientific).

Enzyme-linked immunosorbent assay (ELISA)

Neutrophils were stimulated as above, then suspended in PBS for leukotriene B4 (LTB4) and 5(S)-hydroxyeicosatetraenoic acid (5-HETE) detection. The freeze-thaw process was repeated several times until the cells were fully lysed. The samples were centrifuged for 10 min at 1,500 × *g* at 4°C and the

cell fragments were removed. The supernatant was collected and the assay was performed according to the manufacturer's instructions (Vicmed).

Mouse models

C57 mice, 6–8 weeks old, were purchased from the Xuzhou Medical University Animal Center (Xuzhou, China). All animal procedures were reviewed and approved by the Institutional Animal Care and Use Committee of Xuzhou Medical University (Approval No. 2015090201) in accordance with the U.S. Department of Agriculture, International Association for the Assessment and Accreditation of Laboratory Animal Care, and the National Institutes of Health [NIH] (Bethesda, MD, USA) guidelines.

For the LLC cell and neutrophil co-injection model, 5×10^6 LLC cells/100 μL of PBS with or without 5×10^5 neutrophils were implanted subcutaneously into the backs of male C57 mice. When the tumor volumes were an average size of 40–50 mm^3, 5×10^5 neutrophils in PBS were injected every 3 days for 2 weeks. The control groups were injected with the same volume of PBS. Tumor growth was monitored every other day.

LLC cells (1×10^6) were implanted subcutaneously into both sides of the back in male C57 mice. The LLC cells were allowed to grow to an average size of 40–50 mm^3. The mice were then treated every other day (three treatments). The treatment groups included PBS, neutrophil, and neutrophil incubated with PARP-1 inhibitor (1 μM AG14361 for 1 h) intratumor injections. Primary neutrophils were isolated from the bone marrow *via* gradient centrifugation, according to our previous publication[25]. The injection volume was 30 μL for all treatments. Injections were performed using a syringe with a 31-gauge needle. Tumor growth was monitored every other day. The study was terminated 27 d after the first treatment and the tumors were harvested.

Neutrophil infiltration analysis

The mice were euthanized 15 d after the first treatment and the tumors were processed into a single-cell suspension by shearing the tissue using a 40-μm cell strainer. Neutrophils were stained with different antibodies, including FITC-anti-mouse-Ly-6G (Clone 1A8; Biolegend, San Diego, CA, USA) and APC-anti-mouse-CD11b (Biolegend, San Diego, CA, USA). The samples were analyzed using a FACSCalibur flow cytometer (BD Biosciences, San Jose, CA, USA).

Statistical analysis

All data are presented as the mean ± SEM unless otherwise stated. Statistical analyses were performed using Prism v.7.0 (GraphPad Software, La Jolla, CA, USA). Kaplan–Meier and log-rank tests were used to evaluate the correlation between MPO mRNA expression and survival of lung cancer patients. The significance of the difference between two independent samples was determined using unpaired Student t-tests. One-way ANOVA with Tukey's test was used to compare multiple groups. A $P < 0.05$ was considered statistically significant for all experiments.

Results

Neutrophil infiltration is increased in lung cancer tissues and correlated with a worse prognosis

Neutrophil infiltration influences the progression of most cancers. Kaplan–Meier plotter online analysis[27] was used to determine the relationship between the number of infiltrating neutrophils and overall survival in patients with lung cancer. Multiple factors might affect lung cancer patient survival, such as pathologic and histologic findings, clinical stage, and cigarette smoking history. Therefore, Cox multivariate analysis was selected to evaluate the influence of neutrophil-related genes [*CD11b*, *MPO*, *S100A8*, *S100A9*, and neutrophil elastase (*ELANE*)] on lung cancer patient survival. Based on online data, the histologic findings, tumor stage, cigarette smoking history, and select genes were considered risk factors. According to the results of Cox multivariate analysis, the levels of *CD11b*, *MPO*, *S100A8*, *S100A9*, and *ELANE* expression were negatively correlated with lung cancer prognosis ($P < 0.001$; **Figure 1A–E**), suggesting that the higher the neutrophil infiltration in the tumor tissue, the worse the prognosis. Therefore, we next explored the status of neutrophil infiltration in lung cancer tissues. Seventy-five human lung cancer and paracarcinoma tissues were collected and placed on tissue chips. The IHC results showed that MPO-positive cells showed clear neutrophil-like segmented nuclei, and the infiltrating MPO-positive neutrophil number was clearly increased in lung cancer tissues (**Figure 1F**). Overall, these findings suggest that neutrophil infiltration promotes lung cancer progression, and patients with high neutrophil infiltration in lung cancer tissue have worse survival.

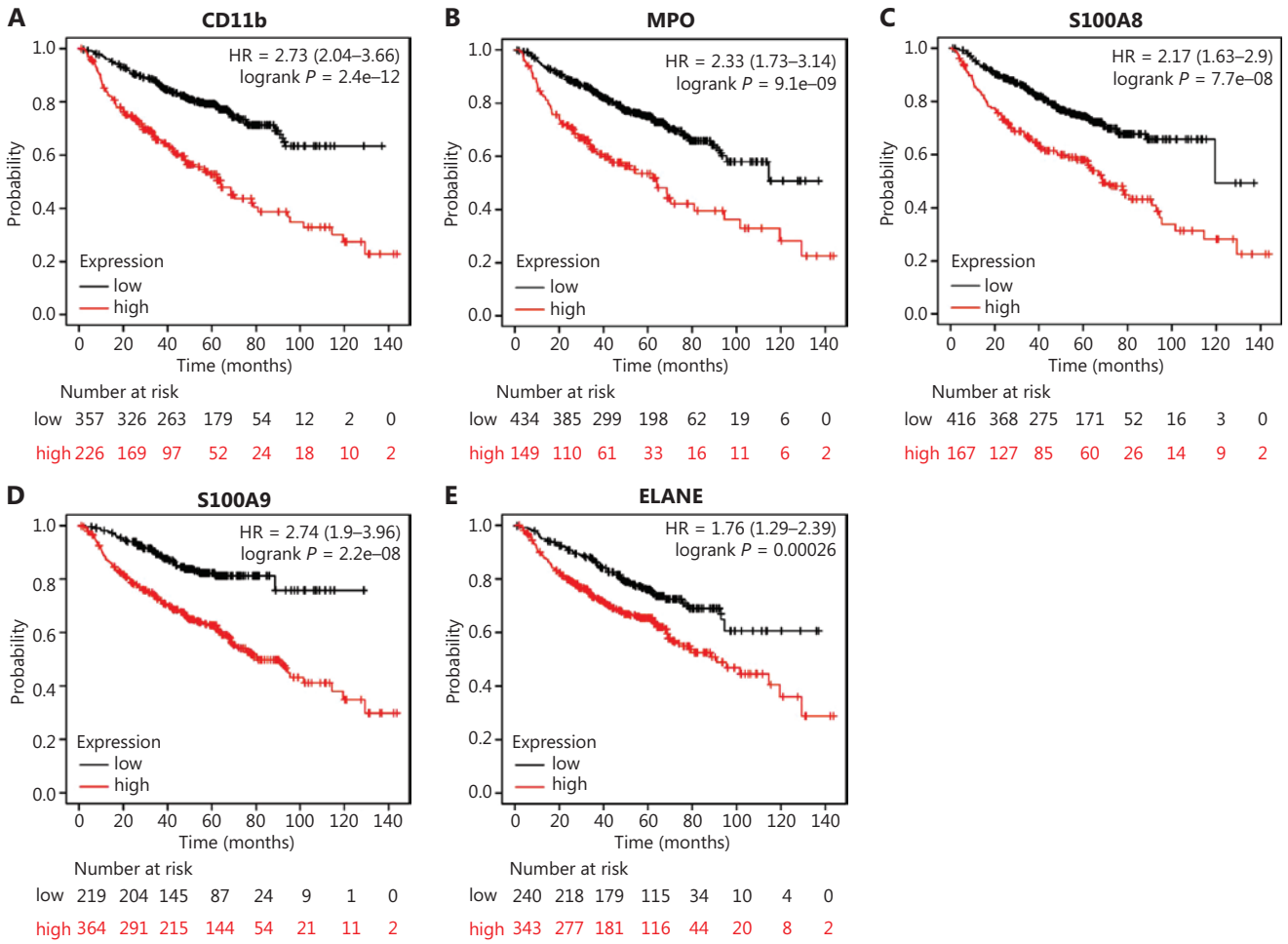
A
CD11b
HR = 2.73 (2.04–3.66)
logrank P = 2.4e–12
Probability
Expression
low
high
Time (months)
Number at risk
low 357 326 263 179 54 12 2 0
high 226 169 97 52 24 18 10 2
B
MPO
HR = 2.33 (1.73–3.14)
logrank P = 9.1e–09
Number at risk
low 434 385 299 198 62 19 6 0
high 149 110 61 33 16 11 6 2
C
S100A8
HR = 2.17 (1.63–2.9)
logrank P = 7.7e–08
Number at risk
low 416 368 275 171 52 16 3 0
high 167 127 85 60 26 14 9 2
D
S100A9
HR = 2.74 (1.9–3.96)
logrank P = 2.2e–08
Number at risk
low 219 204 145 87 24 9 1 0
high 364 291 215 144 54 21 11 2
E
ELANE
HR = 1.76 (1.29–2.39)
logrank P = 0.00026
Number at risk
low 240 218 179 115 34 10 4 0
high 343 277 181 116 44 20 8 2

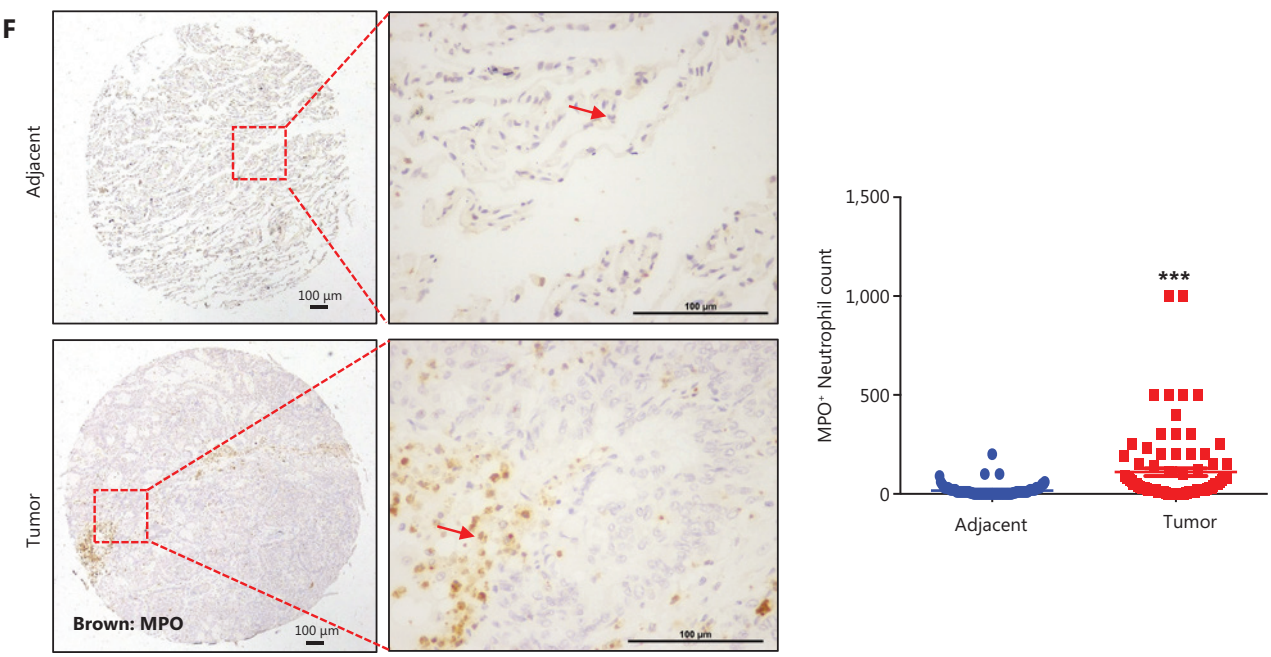
F
Adjacent
Tumor
100 μm
Brown: MPO
MPO+ Neutrophil count
1,500
1,000
500
0
***
Adjacent
Tumor

Figure 1 Infiltrating neutrophils increase in lung cancer tissues and correlate with a worse prognosis. (A–E) Kaplan–Meier survival curves depicting overall survival in lung cancer patients stratified by CD11b (A, $P < 0.001$), MPO (B, $P < 0.001$), S100A8 (C, $P < 0.001$), S100A9 (D, $P < 0.001$), and ELANE (E, $P < 0.001$) expression in lung cancer tissues analyzed by Cox multivariate analysis. (F) Representative immunohistochemistry images of MPO expression in human lung cancer and para-carcinoma tissues ($n = 75$, $P < 0.001$). Scale bar: 100 μm.

Cancer-educated neutrophils promote lung cancer cell invasion, migration, and proliferation and lung cancer growth

Neutrophil activation releases potent antimicrobial factors that lead to tissue inflammation[28]. Additionally, cancers are inflammatory diseases, and cancer tissue-infiltrated neutrophils are educated and more activated[9]. Therefore, to determine how these activated neutrophil-released factors influence the invasion, migration, and proliferation of lung cancer cells, we treated two human lung cancer cell lines (A549 and H1299 cells) with serum-free media conditioned by HL-60 cell-differentiated neutrophil activation as neutrophil-activated productions. Neutrophil-activated production effectively promoted A549 and H1299 cell invasion, migration, and proliferation tested based on Transwell and CCK-8 assay findings (**Figure 2A–D**). Furthermore, the BMNs from wild-type mice were used to prepare neutrophil-activated production. The activated neutrophils promoted mouse LLC cell invasion and migration (**Figure S1A**). Next, the neutrophils from diverse sources were educated by co-culturing separately with A549, H1299, or LLC cells. N2 markers (*ccl5*,

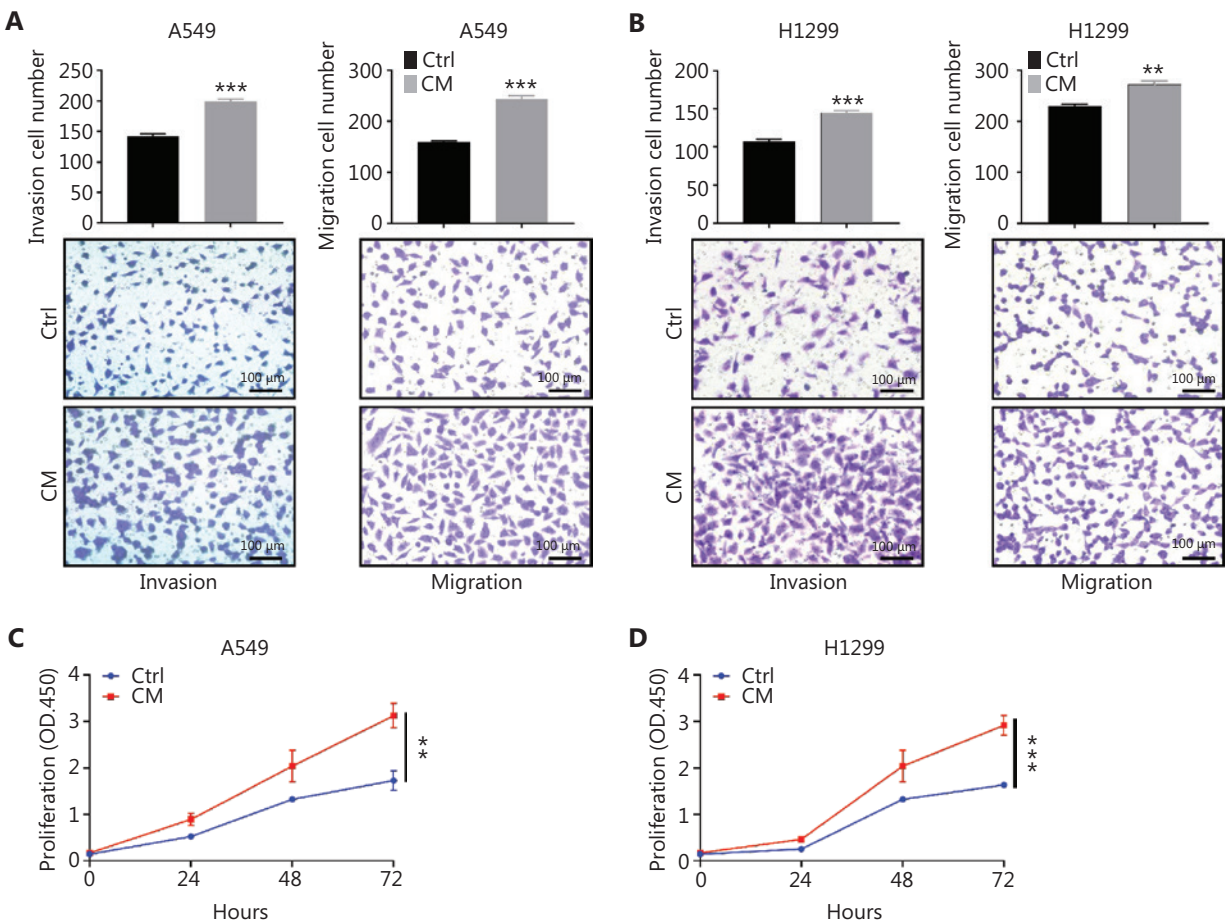

Figure 2 Continued

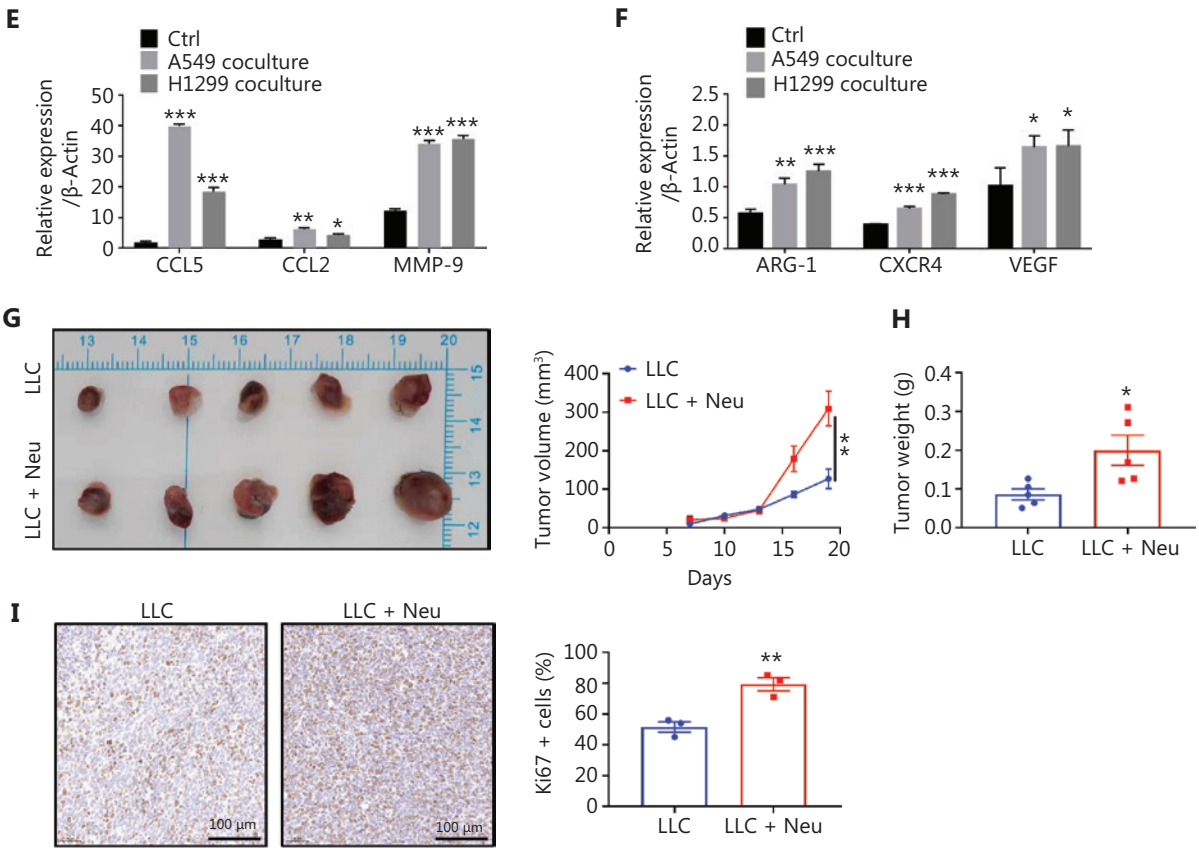

Figure 2 Cancer-educated neutrophils promote lung cancer cell invasion, migration, and proliferation and lung cancer growth. (A and B) HL-60 cell-differentiated neutrophil-activated production (50 μL) was added to the Transwell upper chamber to stimulate (A) A549 and (B) H1299 cells. Then, the invading and migrating cell numbers were analyzed (CM, condition medium as neutrophil-activated productions). (C and D) The proliferation of lung cancer cells was assessed by CCK-8 assays in A549 and H1299 cells treated with CM or control medium for different times (0, 24, 48, and 72 h). (E and F) *Ccl5*, *ccl2*, *mmp-9*, *arg-1*, *cxcr4*, and *vegf* mRNA in neutrophils co-cultured with A549 or H1299 cells were measured by real-time PCR. (G) 5×10^6 LLC was subcutaneously injected into the back of each mouse with or without BMN (Neu, 5×10^5) co-injection. The tumor volume was monitored. (H) Tumor weight. (I) Representative pictures of Ki67 IHC staining in paraffin-embedded tumor tissues. Quantification of the percentage of Ki67-positive cells within tumor tissues. Scale bar: 100 μm. All data are expressed as the mean ± SEM (n = 3–5). *P < 0.05, **P < 0.01, ***P < 0.001.

ccl2, *mmp-9*, *arg-1*, *cxcr4*, and *vegf* mRNA) were significantly increased in co-cultured neutrophils, indicating that lung cancer cells promote neutrophil conversion to a pro-tumor type (**Figure 2E, F and Figure S1B**). These results demonstrated that lung cancer cells induce neutrophil activation and activated neutrophils promote lung cancer cell motility and proliferation *in vitro*.

We further determined the effect of neutrophils on lung cancer progression in an *in vivo* mouse model. Notably, tumor volume and weight increased significantly when LLC cells were co-injected with neutrophils compared with LLC cell saline injection (**Figure 2G and H**). Furthermore, Ki67 staining was performed to confirm the ability of neutrophils to promote proliferation. The results showed that neutrophil injection dramatically increased the percentage of Ki67-positive hyperproliferative lung cancer cells (from 51.67% ± 5.86% to 79.33% ± 7.37%; $P < 0.05$, **Figure 2I**).

Neutrophil-released MMP-9 promotes lung cancer cell invasion, migration, and proliferation

Our findings indicated that tumor-educated neutrophils release factors that promote lung cancer cell invasion,

migration, and proliferation. The real-time PCR results also suggested that MMP-9 mRNA levels are increased in neutrophils co-cultured with A549, H1299, or LLC cells. Furthermore, MMP-9 is highly expressed in tumor tissues and has a crucial role in cancer cell migration, invasion, and angiogenesis[29,30]. Tumor-associated neutrophils represent an important source of MMP-9 in lung cancer[31]. Therefore, to determine whether neutrophil promotion of lung cancer progression is dependent on MMP-9, a MMP-specific inhibitor (1.10PE) was applied during neutrophil activation. The results showed that the MMP-9 inhibitor effectively blocked lung cancer cell invasion, migration, and proliferation promoted by neutrophil-activated productions (**Figure 3A–D and Figure S2**). Next, the inhibitor was used in a neutrophil and lung cancer cell co-culture Transwell system, and similar results were observed (**Figure 3E and F**). These results suggest that MMP-9 is the key factor promoting lung cancer progression in lung cancer-educated neutrophils.

PARP-1 regulates MMP-9 expression and neutrophil-induced lung cancer cell invasion, migration, and proliferation

Our previous study showed that a PARP-1 inhibitor attenuated the acute lung inflammation promoted by neutrophil recruitment[20]. We explored the relationship between PARP-1 and tumor-educated neutrophils involved in MMP-9 release. The results showed that PARP-1 expression was markedly increased in neutrophils activated by A549 or H1299 cells

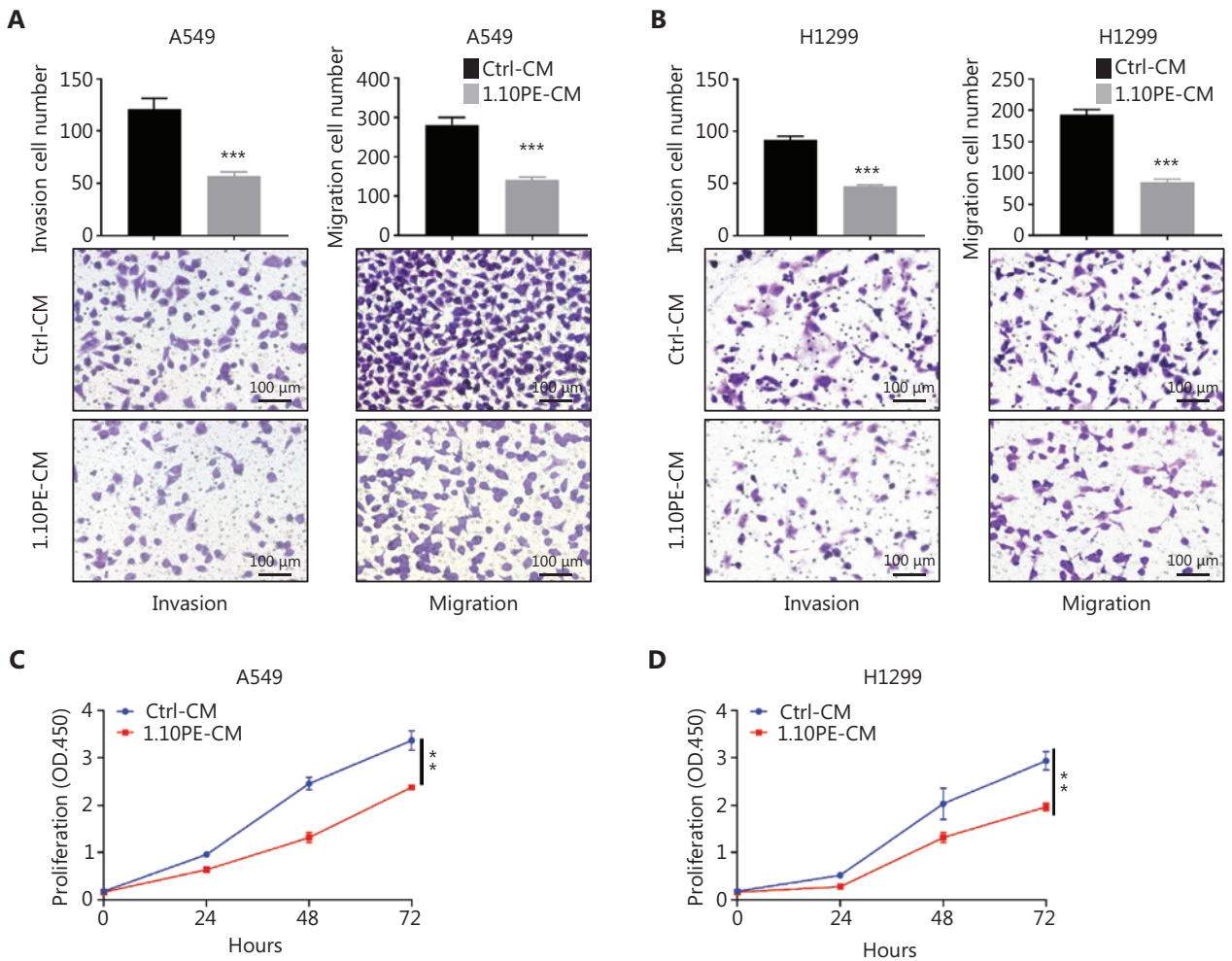

Figure 3 Continued

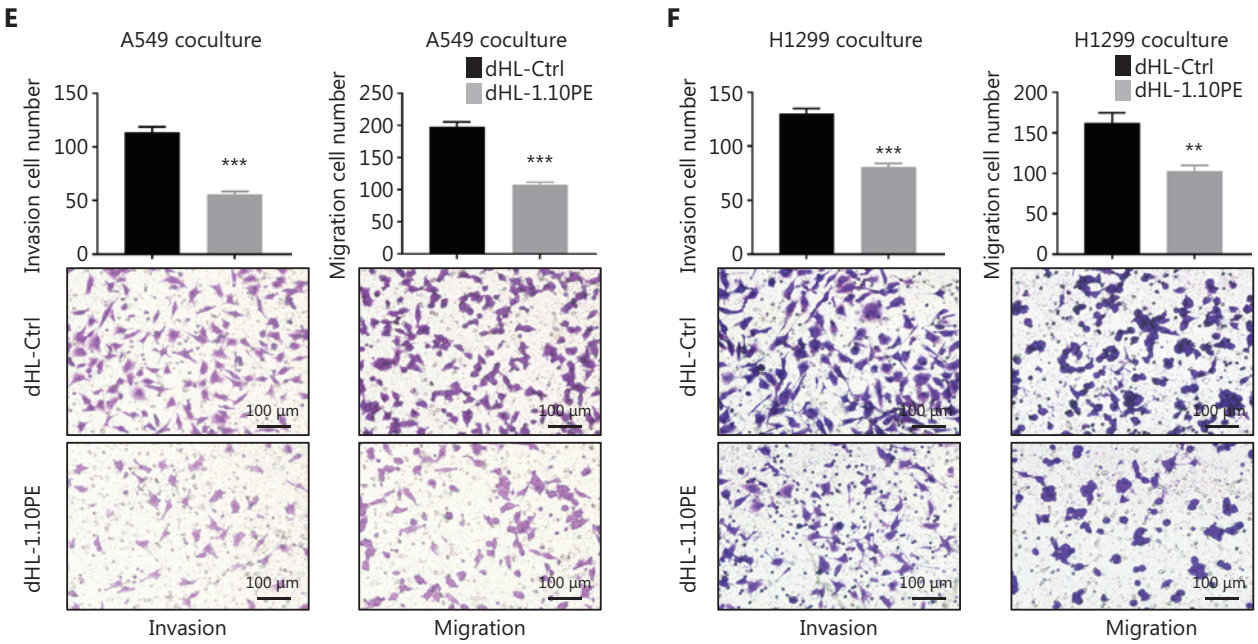

Figure 3 Neutrophil-released MMP-9 promotes lung cancer cell invasion, migration, and proliferation. (A and B) 1.10PE (200 μM) was applied during HL-60 cell-differentiated neutrophil activation. Then, the neutrophil-activated productions (Ctrl-CM, 50 μL) with or without 1.10PE (1.10PE-CM) were added to the Transwell upper chamber to stimulate A549 (A) and H1299 cells (B). Then, the invading and migrating cell numbers were analyzed. (C and D) The proliferation of lung cancer cells was assessed by CCK-8 assays in A549 and H1299 cells treated with neutrophil-activated productions with or without 1.10PE for different times (0, 24, 48, and 72 h). (E and F) The neutrophils (dHL-Ctrl, 6×10^6 in 600 μL of serum-free medium) were pre-seeded for the co-culture Transwell system in the lower chamber with or without 1.10PE (dHL-1.10PE). Then, A549 (E) or H1299 cells (F) were seeded in the upper chamber. The invading and migrating cell numbers were analyzed. Scale bar: 100 μm. All data are expressed as the mean ± SEM (n = 5). $^{**}P < 0.01$, $^{***}P < 0.001$.

(**Figure S3A and B**). Then, shRNA was used to knock-down PARP-1 in a neutrophil-like cell line (dHL-60; **Figure S3C**). MMP-9 activity and expression were significantly decreased in PARP-1 knock-down neutrophils stimulated by LPS for 4 h (**Figure 4A and B**). Next, the neutrophils were co-cultured with A549 or H1299 cells and the activated neutrophil MMP-9 expression also decreased when PARP-1 was knocked down (**Figure 4C and D**), indicating that PARP-1 regulates MMP-9 expression in tumor-educated neutrophils.

We further determined if PARP-1 could mediate neutrophil promotion of lung cancer cell mobility and proliferation. Lung cancer cell invasion, migration, and proliferation were reversed by PARP-1 knock-down or when the PARP-1 inhibitor, AG14361, was administered (**Figure 4E–H and Figure S3D**). Similar results were observed in the neutrophil and lung cancer cell co-culture Transwell system (**Figure S3E and F**). Overall, PARP-1 regulates neutrophil activation and promotes lung cancer cell invasion, migration, and proliferation *via* MMP-9 expression and release.

PARP-1 binding to ALOX5 mediates MMP-9 expression in neutrophils

To further investigate how PARP-1 mediates MMP-9 expression in neutrophils educated by lung cancer cells, IP/MS was used to identify PARP-1 binding proteins related to MMP-9 expression in A549-educated neutrophils. As shown in **Table S2 and Figure S4A**, among these PARP-1 interacting proteins, the metabolites of ALOX5, including LTB4 and 5-HETE, promoted MMP-9 production by activating ERK and p38 MAPK signaling[32-35]. ALOX5, LTB4, and 5-HETE expression increased in activated neutrophils and the expression was reduced when PARP-1 was knocked down (**Figure 5A and Figure S4B–E**). An ALOX5 inhibitor, Zileuton, blocked MMP-9 expression in activated neutrophils (**Figure 5B**). A co-IP assay confirmed that PARP-1 is directly bound to ALOX5 and that the binding of PARP-1 to ALOX5 was upregulated during neutrophil activation (**Figure 5C and D**). As expected, the same result was observed in neutrophils

educated by lung cancer cells (**Figure S4F–G**). Moreover, to explore the binding capacity of PARP-1 and ALOX5 directly, Flag-PARP-1 and HA-ALOX5 plasmids were transfected into 293T cells. After co-transfection, ALOX5 was immunoprecipitated by anti-Flag antibody but not by the control IgG antibody (**Figure S4H**). To illustrate whether the PARylation of ALOX5 was also changed upon lung cancer education, we immunoprecipitated ALOX5 and blotted with a PAR antibody. PARylation of ALOX5 was increased in stimulated neutrophils and PARylation of ALOX5 was inverted when PARP-1 was knocked down (**Figure S4I–J**). These results suggest that PARylation of ALOX5 by PARP-1 increased protein stabilization. Importantly, Zileuton effectively blocked lung cancer cell invasion, migration, and proliferation promoted by neutrophil-activated productions (**Figure 5E–H and Figure S4K**). Next, the inhibitor was used in a neutrophil and lung cancer cell co-culture Transwell system, and similar results were obtained (**Figure S4L and M**). These results indicate that PARP-1-induced MMP-9 expression promotes lung cancer cell invasion, migration, and proliferation by interacting and stabilizing ALOX5 with PARylation modification.

Blocking neutrophil PARP-1 inhibits lung cancer progression in mice

We next determined if neutrophil-specific PARP-1 blocking can rescue neutrophil-promoted lung cancer progression. The PARP-1 inhibitor, AG14361, was used in an LLC model. Two of 24 mice were excluded because the lung cancer model failed to be established. Tumor growth measured by tumor volume, weight, and Ki67 staining increased significantly when LLC cells were co-injected with neutrophils compared with PBS as a control (**Figure 6A–C**). Moreover, neutrophil-induced tumor growth was attenuated significantly when co-injected neutrophils were pre-incubated with AG14361, which depleted intratumoral neutrophil infiltration (**Figure 6A–D**). Additionally, AG14361 was injected intraperitoneally into LLC mice. The results showed that AG14361 intraperitoneal

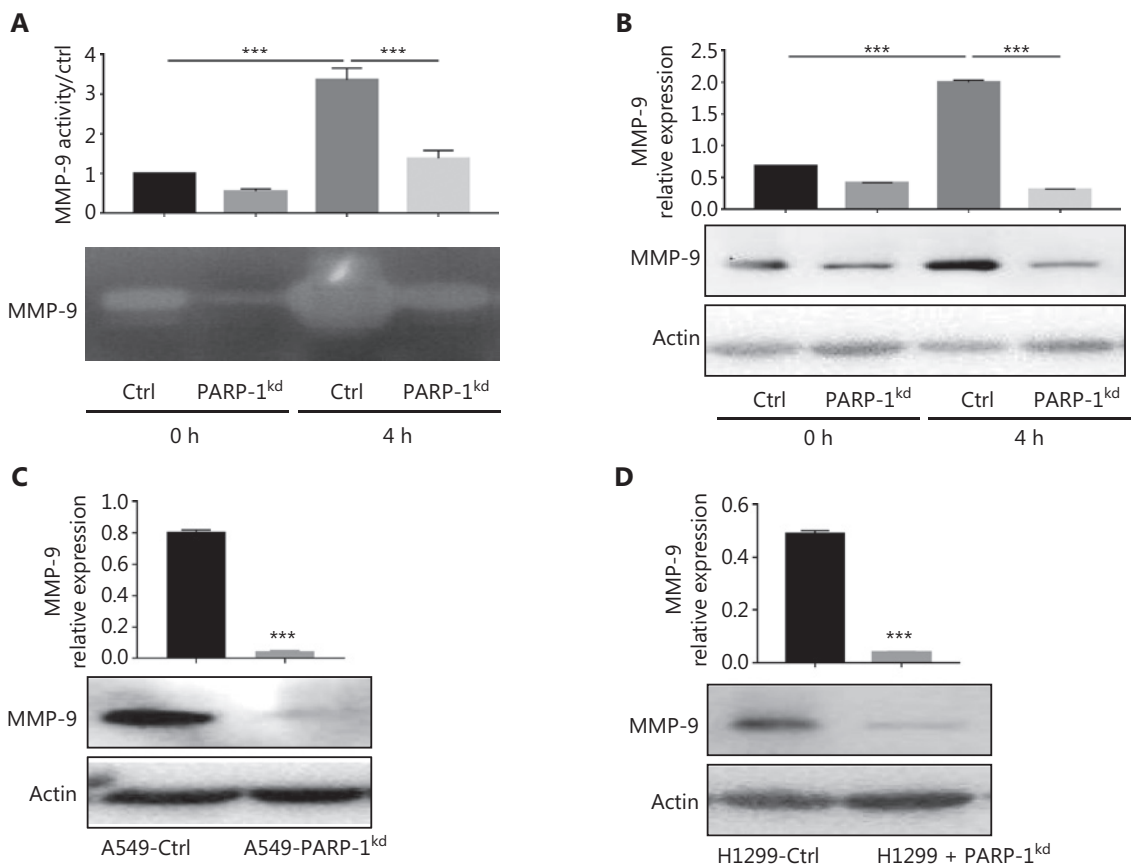

Figure 4 Continued

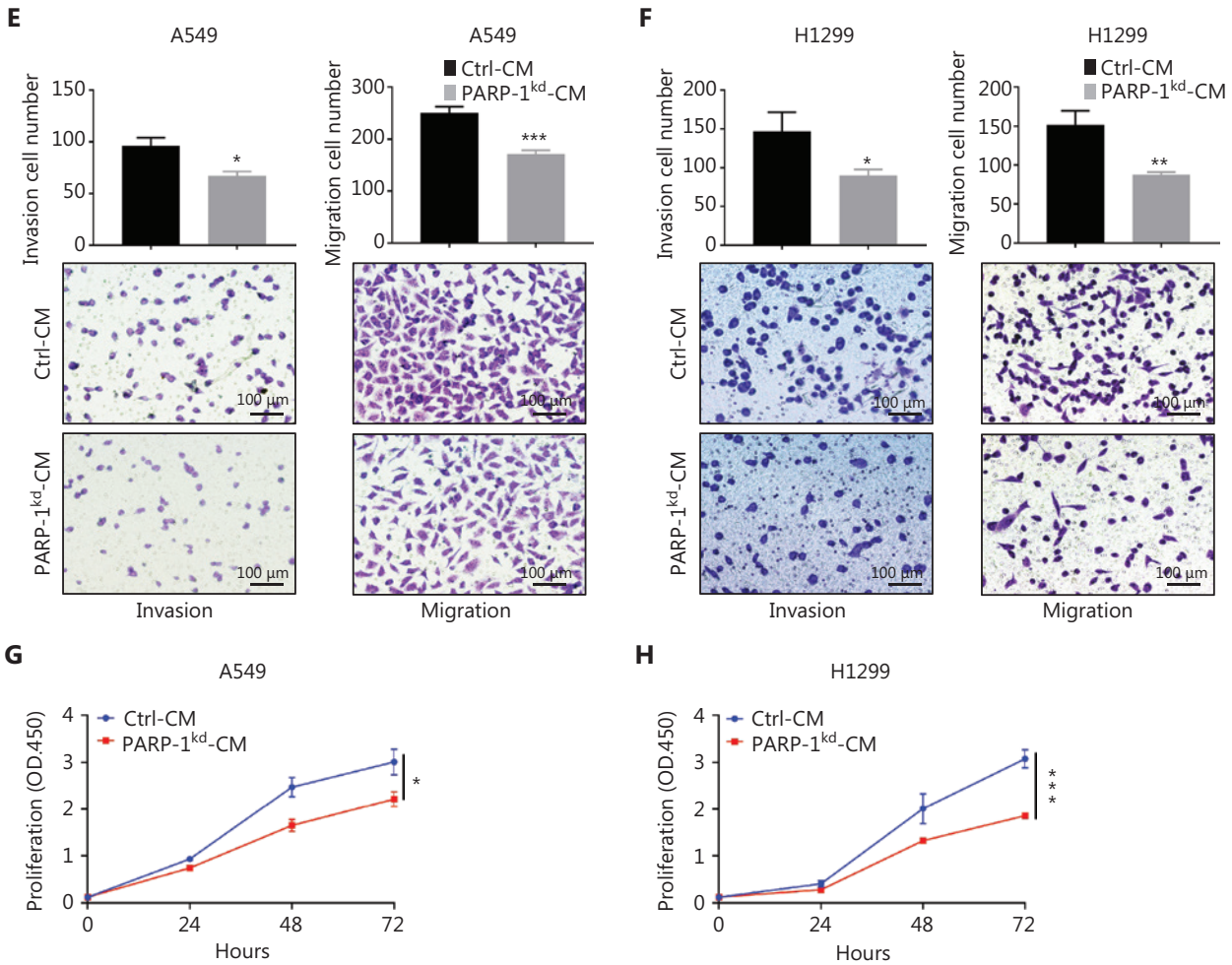

Figure 4 PARP-1 regulates MMP-9 expression and neutrophil-induced lung cancer cell invasion, migration, and proliferation. (A) LPS stimulated normal or PARP-1 knock-down (PARP-1^{kd}) HL-60 cell-differentiated neutrophils for 4 h. MMP-9 enzyme activity was measured with a gelatin zymography assay. (B) MMP-9 protein expression was measured by western blot, with actin used as the internal control. (C and D) Normal or PARP-1 knocked-down HL-60 cell-differentiated neutrophils were co-cultured with A549 or H1299 cells. Then, MMP-9 protein expression was measured by western blot, with actin used as the internal control. (E and F) Normal (Ctrl-CM) or PARP-1 knocked-down HL-60 cell-differentiated neutrophil-activated productions (PARP-1^{kd} -CM, 50 μL) were added to the Transwell upper chamber to stimulated (E) A549 and (F) H1299 cells. Then, the invading and migrating cell numbers were analyzed. Scale bar: 100 μm. (G and H) The proliferation of lung cancer cells was assessed by CCK-8 assays in A549 and H1299 cells treated with normal (Ctrl-CM) or PARP-1 knocked-down neutrophil-activated populations (PARP-1^{kd}-CM) for different times (0, 24, 48, and 72 h). All data are expressed as the mean ± SEM (n = 3–5). *P < 0.05, **P < 0.01, ***P < 0.001.

injection significantly inhibited lung cancer growth (**Figure 6E–G**). These results demonstrate an important role of PARP-1 in neutrophil-induced lung cancer progression, which can be reversed by AG14361 in mice.

Discussion

In addition to traditional treatments, such as surgery and radiotherapy, emerging targeted therapy and immunotherapy have provided new strategies for lung cancer, but the overall therapeutic efficacy remains unsatisfactory. The leading cause of treatment failure and death in lung cancer patients is resistance to the treatment drug[36]. Unlike tumor cells but like immune cells, such as neutrophils, stromal cells within the tumor microenvironment are genetically stable and represent an attractive therapeutic target because stromal cells are less likely to develop drug resistance[37]. Therefore, understanding the molecular mechanism underlying lung cancer-educated

neutrophil activation and identifying effective molecular targets is of great theoretical and practical significance. In this study we first found that PARP-1 regulates neutrophil MMP-9 expression by binding to ALOX5, thus affecting lung cancer growth. A PARP-1 inhibitor effectively reversed the lung cancer progression promoted by neutrophils, which provides a new target and strategy for clinical anti-stromal cell therapy for lung cancer patients.

As a chronic inflammatory disease[38], several studies have shown that neutrophil infiltration of lung cancer tissues is increased and infiltrating neutrophils remain in highly activated states and exhibit tumor-promoted phenotypes[9,39]. On a clinical level we confirmed that the number of neutrophils was increased in lung cancer tissues and neutrophil infiltration promoted lung cancer progression. Patients with high neutrophil infiltration of lung cancer tissues had worse survival. We showed that tumor growth increased significantly when LLC cells were co-injected with neutrophils into mice *in vivo*. Furthermore, we found that lung neutrophils remained in highly activated states by cancer cell education. MMP-9 expression and activity were increased in activated neutrophils and 1.10 PE effectively blocked lung cancer cell invasion and migration promoted by neutrophil-activated production. This finding suggests that activated neutrophil-released MMP-9 has a key role in lung cancer progression. This finding is consistent with the findings of another study that showed MMP-9 is highly expressed in lung cancer tissues and neutrophil infiltrating the tumor are an important source of MMP-9[31].

In agreement with our previous report, a PARP-1 inhibitor clearly attenuated LPS-induced acute lung inflammation promoted by neutrophil recruitment[20]. We also found that PARP-1 expression was increased in neutrophils educated by lung cancer cells, indicating that PARP-1 mediates neutrophil activation induced by lung cancer cells. PARP-1 knock-down

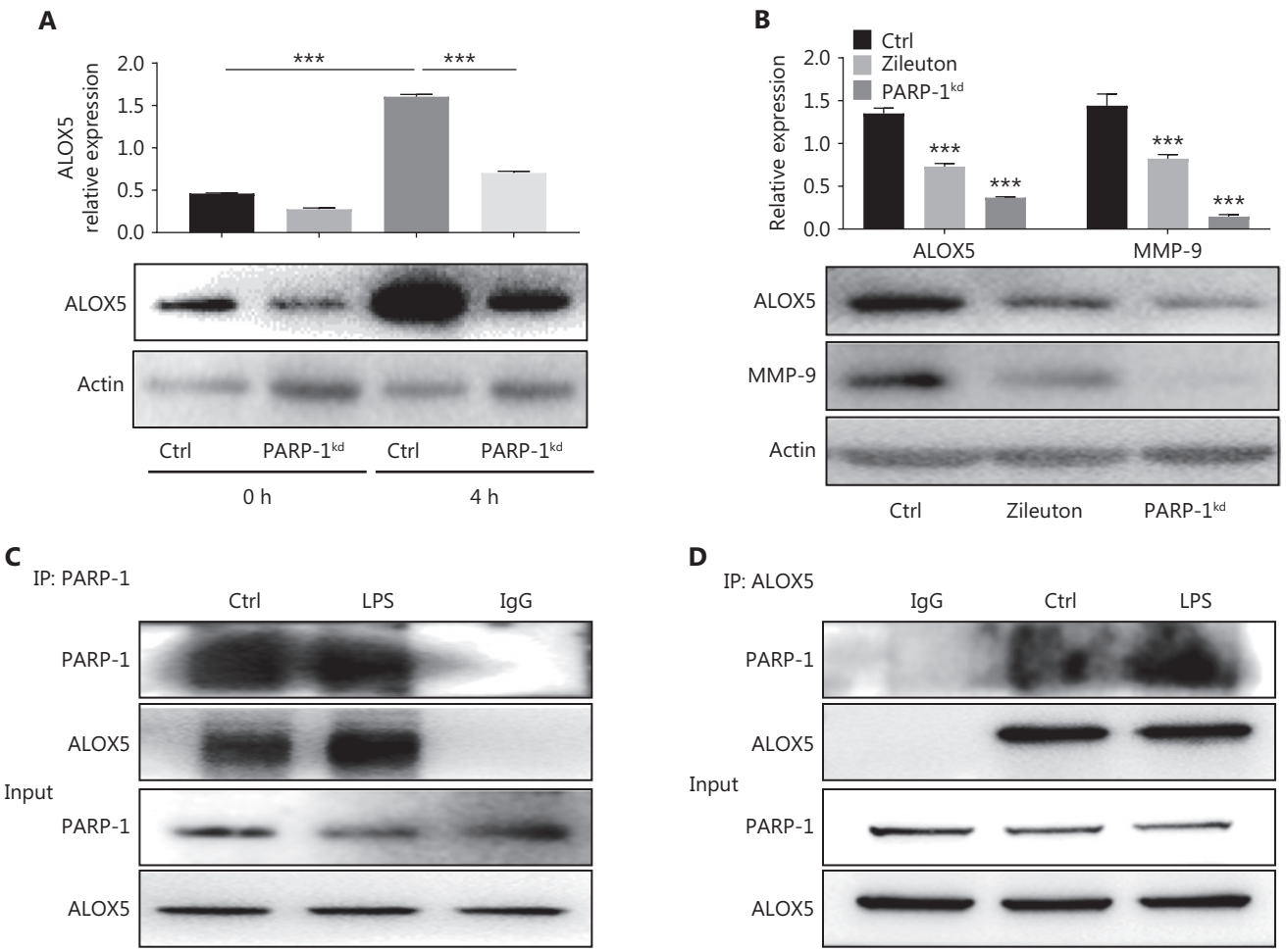

Figure 5 Continued

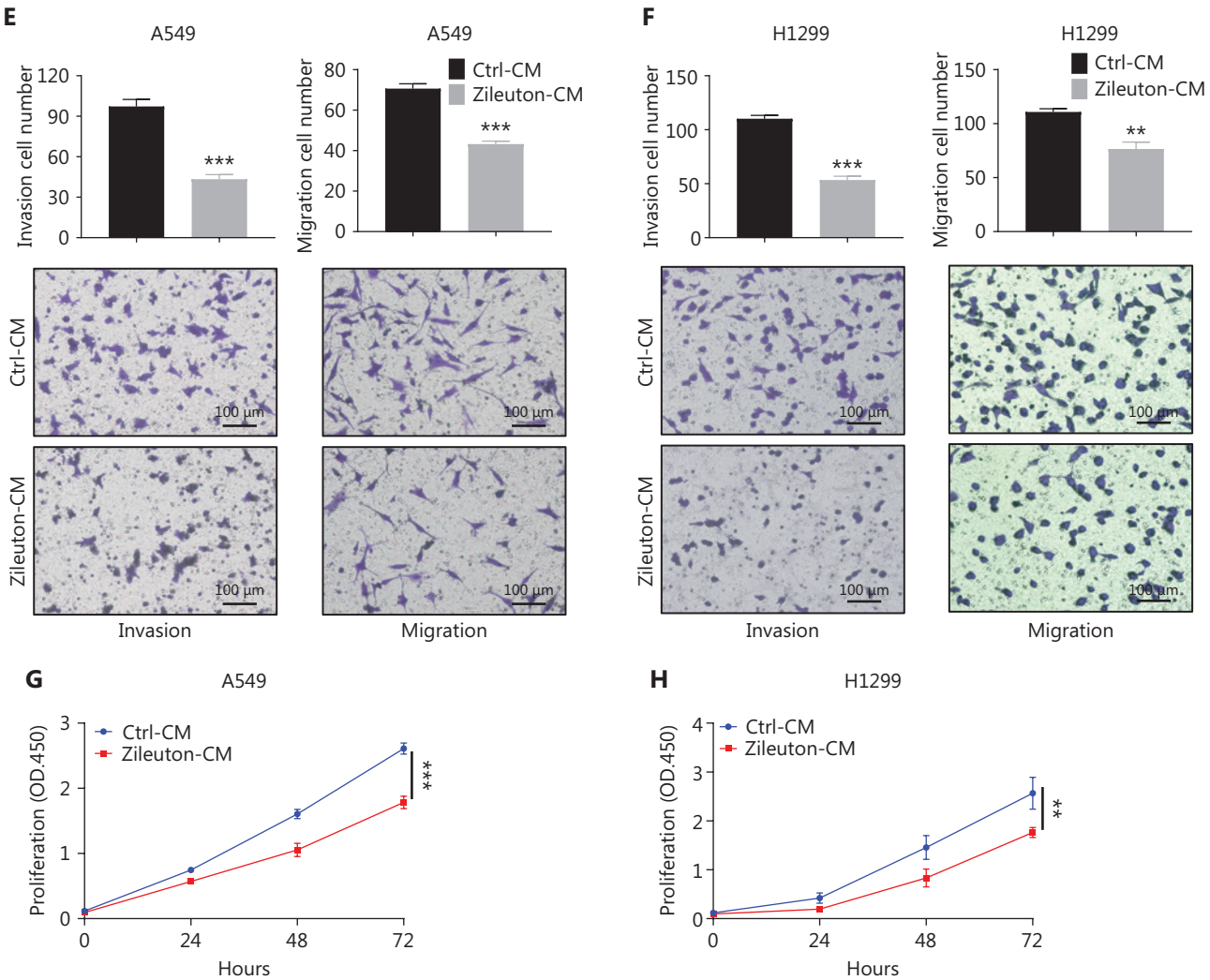

Figure 5 PARP-1 binding to ALOX5 mediates MMP-9 expression in neutrophils. (A) LPS stimulated normal or PARP-1 knocked-down HL-60 cell-differentiated neutrophils for 4 h. ALOX5 protein expression was measured by western blot, with actin as the internal control. (B) ALOX5 and MMP-9 protein expression was measured by western blot, with actin used as the internal control. (C and D) Co-immunoprecipitation of PARP-1 with ALOX5 in neutrophils. (E and F) Zileuton (50 μM) was used during HL-60 cell-differentiated neutrophil activation. Then, the neutrophil-activated productions (Ctrl-CM, 50 μL) with or without Zileuton (Zileuton-CM) were added to the Transwell upper chamber to stimulate (E) A549 and (F) H1299 cells. Then, the invading and migrating cell numbers were analyzed. Scale bar: 100 μm. (G and H) The proliferation of lung cancer cells was assessed by CCK-8 assays in A549 and H1299 cells treated with neutrophil-activated productions with or without Zileuton for different times (0, 24, 48, and 72 h). All data are expressed as the mean ± SEM (n = 3–5). $^{**}P < 0.01$, $^{***}P < 0.001$.

in neutrophils reversed the high MMP-9 expression and lung cancer cell invasion and migration. IP/MS was used to identify PARP-1 binding proteins related to MMP-9 expression in lung cancer cell-activated neutrophils to further explore the underlying mechanisms. ALOX5 was bound to PARP-1 with high affinity. A previous study suggested that metabolites of ALOX5, including LTB4 and 5-HETE, promote MMP-9 production by activating ERK and p38 MAPK signaling[32-35]. Additionally, lung cancer cell-induced upregulation of LTB4 and 5-HETE in neutrophils was significantly blocked by downregulating PARP-1 expression. To explore the underlying molecular mechanism, the co-IP results confirmed that PARP-1 bound to ALOX5 and binding of PARP-1 to ALOX5 was upregulated during lung cancer cell stimulation. PARylation of ALOX5 was increased in stimulated neutrophils, and PARylation of ALOX5 was reversed when PARP-1 was knocked down. Knock-down

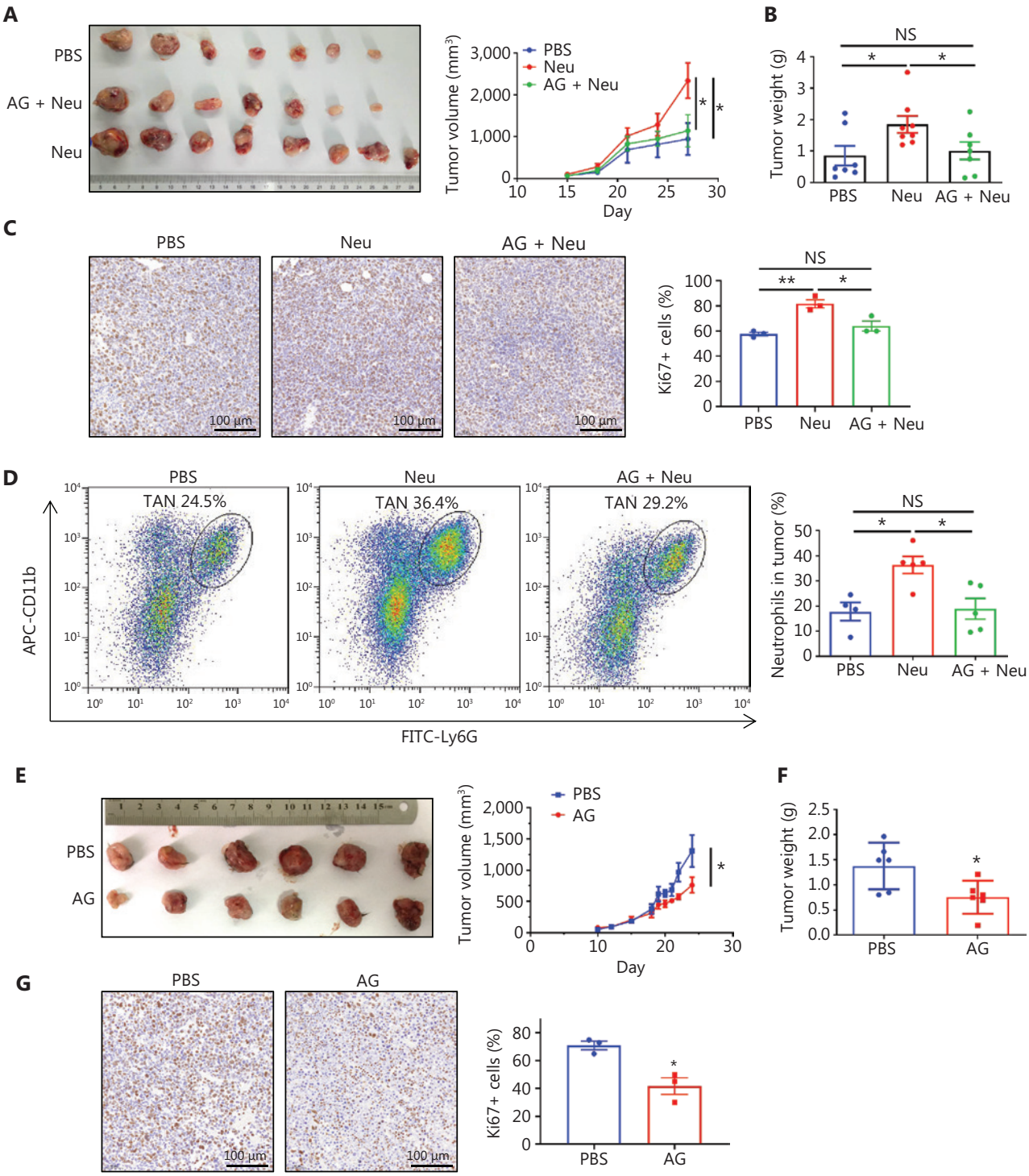

Figure 6 Blocking neutrophil PARP-1 inhibits lung cancer progression in mice. (A) LLC cells were injected subcutaneously with PBS, mouse neutrophils (Neu), or AG14361 (AG) and Neu. The tumor volumes were monitored. (B) Tumor weights. (C) Representative pictures of Ki67 IHC staining in paraffin-embedded tumor tissues. Quantification of the percentage of Ki67-positive cells within tumor tissues. (D) Neutrophils (marked by CD11b and Ly6G antibody) in tumor tissues were measured by flow cytometry. (E) LLC cells were injected subcutaneously. Then, AG14361 or PBS was injected intraperitoneally 5 times. The tumor volumes were monitored. (F) Tumor weights. (G) Representative pictures of Ki67 IHC staining in paraffin-embedded tumor tissues. Quantification of the percentage of Ki67-positive cells within tumor tissues. Scale bar: 100 μm. All data are expressed as the mean ± SEM (n = 5–8). *P < 0.05, NS, not significant.

of PARP-1 in neutrophils reduced PARylation of ALOX5 and ALOX5 protein levels, indicating that PARylation of ALOX5 by PARP-1 increased protein stabilization. Furthermore, Zileuton administration significantly inhibited activated neutrophil MMP-9 expression and neutrophil-promoted lung cancer cell invasion and migration, indicating that ALOX5 enhances MMP-9 expression in neutrophils. Whether the regulatory mechanism underlying the ALOX5 and MMP-9 interaction is also 5-HETE- and LTB4-dependent requires further investigation in activated neutrophils. These findings suggest a distinct neutrophil activation mechanism underlying PARP-1-ALOX5-mediated MMP-9 expression in lung cancer progression (**Figure 7**).

From a therapeutic perspective, cancer patients have poor autoimmunity and are often at risk for infections, thus complete depletion of neutrophils may have a negative impact on immune function[40]. This study suggested that specific blocking of neutrophil PARP-1 significantly inhibits lung cancer progression in mice. Therefore, based on the literature and our results, we propose a lung cancer treatment strategy that targets the tumor-specific neutrophil PARP-1 gene to attenuate the promotion of lung cancer metastasis by neutrophils. Moreover, as mentioned above, unlike tumor cells but like immune cells, stromal cells within the tumor microenvironment are genetically stable and represent an attractive therapeutic target because stromal cells are less likely to develop drug resistance[37]. Developing a neutrophil-specific target PARP-1 inhibitor is an important advance. We have developed a neutrophil-specific target nanoparticle system based on human serum albumin for cancer therapy[26]. Therefore, the combination of both PARP-1 inhibitor and neutrophil-specific target nanoparticle will be investigated as a novel lung cancer treatment in a corollary study.

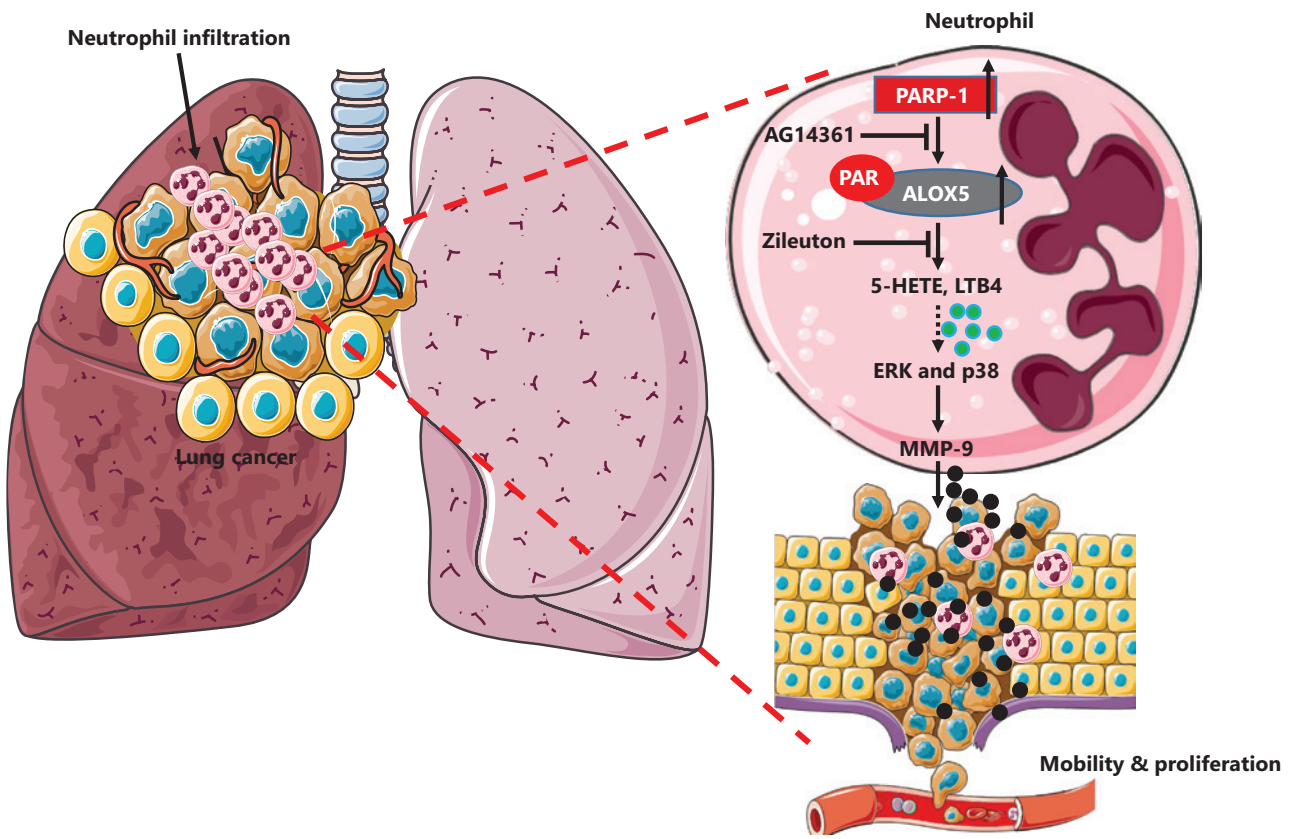

Figure 7 Schematic of neutrophil PARP-1-ALOX5-mediated MMP-9 in lung cancer. Infiltrated neutrophils are increased in lung cancer tissues and negatively correlated with the prognosis of patients. After neutrophils are exposed to lung cancer cells, PARP-1 interacts with ALOX5 and enhances protein stabilization through PARylation of ALOX5. Increasing ALOX5 metabolites promotes MMP-9 production *via* activation of ERK and p38 MAPK pathways. Blocking PARP-1 by AG14361 or ALOX5 by Zileuton reduces MMP-9 production and mitigates neutrophil-mediated lung cancer progression.

Conclusions

In summary, this study provides novel insight into PARP-1-mediated neutrophil activation, which promotes the development of lung cancer. During this process, lung cancer increases neutrophil activation and enhances PARP-1 expression and regulates ALOX5 PARylation and stabilization, mediating MMP-9 expression and release. Therapeutic targeting of the PARP-1 signaling pathway may represent an innovative approach to treating neutrophil-promoted lung cancer.

Grant support

This work was supported by grants from the National Key R&D Program of China (Grant No. 2018YFA0900900), the National Natural Science Foundation of China (Grant Nos. 82273334, 82203172, 81871869, and 81400055), the Jiangsu Province Social Development Key Projects (Grant Nos. BE2020641 and BE2020640), the Xuzhou Medical University Excellent Talent Research Start-up Fund (Grant No. RC20552157), and the Jiangsu Province Capability Improvement Project through Science, Technology and Education (Grant No. CXZX202234). The project was funded by the China Postdoctoral Science Foundation (Grant No. 2023M732970).

Conflict of interest statement

No potential conflicts of interest are disclosed.

Author contributions

Conceived and designed the analysis: Lulu Han, Junnian Zheng, Gang Wang.
Collected the data: Lulu Han, Yuxin Chen, Nan Huang, Xiaowan Zhou, Yanfang Lv.
Contributed data or analysis tools: Yanfang Lv, Huizhong Li, Dafei Chai.
Performed the analysis: Lulu Han, Yuxin Chen.
Wrote the paper: Lulu Han, Gang Wang.

Data availability statement

The data generated in this study are available upon request from the corresponding author.

References

1. Sung H, Ferlay J, Siegel RL, Laversanne M, Soerjomataram I, Jemal A, et al. Global cancer statistics 2020: GLOBOCAN estimates of incidence and mortality worldwide for 36 cancers in 185 countries. CA Cancer J Clin. 2021; 71: 209-49.
2. Cao M, Li H, Sun D, He S, Yan X, Yang F, et al. Current cancer burden in china: epidemiology, etiology, and prevention. Cancer Biol Med. 2022; 19: 1121-38.
3. Kargl J, Busch SE, Yang GH, Kim KH, Hanke ML, Metz HE, et al. Neutrophils dominate the immune cell composition in non-small cell lung cancer. Nat Commun. 2017; 8: 14381.
4. Ilie M, Hofman V, Ortholan C, Bonnetaud C, Coelle C, Mouroux J, et al. Predictive clinical outcome of the intratumoral CD66b-positive neutrophil-to-CD8-positive T-cell ratio in patients with resectable nonsmall cell lung cancer. Cancer. 2012; 118: 1726-37.
5. Schernberg A, Mezquita L, Boros A, Botticella A, Caramella C, Besse B, et al. Neutrophilia as prognostic biomarker in locally advanced stage III lung cancer. PLoS One. 2018; 13: e0204490.
6. Mandaliya H, Jones M, Oldmeadow C, Nordman II. Prognostic biomarkers in stage IV non-small cell lung cancer (NSCLC): neutrophil to lymphocyte ratio (NLR), lymphocyte to monocyte ratio (LMR), platelet to lymphocyte ratio (PLR) and advanced lung cancer inflammation index (ALI). Transl Lung Cancer Res. 2019; 8: 886-94.
7. Shaul ME, Eyal O, Guglietta S, Aloni P, Zlotnik A, Forkosh E, et al. Circulating neutrophil subsets in advanced lung cancer patients exhibit unique immune signature and relate to prognosis. FASEB J. 2020; 34: 4204-18.
8. Russo A, Russano M, Franchina T, Migliorino MR, Aprile G, Mansueto G, et al. Neutrophil-to-lymphocyte ratio (NLR), platelet-to-lymphocyte ratio (PLR), and outcomes with nivolumab in pretreated non-small cell lung cancer (NSCLC): a large retrospective multicenter study. Adv Ther. 2020; 37: 1145-55.
9. Hedrick CC, Malanchi I. Neutrophils in cancer: heterogeneous and multifaceted. Nat Rev Immunol. 2022; 22: 173-87.
10. Chen S, Zhang Q, Lu L, Xu C, Li J, Zha J, et al. Heterogeneity of neutrophils in cancer: one size does not fit all. Cancer Biolo Med. 2022; 19: 1629-48.
11. Pylaeva E, Korschunow G, Spyra I, Bordbari S, Siakaeva E, Ozel I, et al. During early stages of cancer, neutrophils initiate anti-tumor immune responses in tumor-draining lymph nodes. Cell Rep. 2022; 40: 111171.
12. Masucci MT, Minopoli M, Carriero MV. Tumor associated neutrophils. Their role in tumorigenesis, metastasis, prognosis and therapy. Front Oncol. 2019; 9: 1146.
13. Xue RD, Zhang QM, Cao Q, Kong RR, Xiang X, Liu HK, et al. Liver tumour immune microenvironment subtypes and neutrophil heterogeneity. Nature. 2022; 612: 141-7.
14. Gong Z, Li Q, Shi J, Li P, Hua L, Shultz LD, et al. Immunosuppressive reprogramming of neutrophils by lung mesenchymal cells promotes breast cancer metastasis. Sci Immunol. 2023; 8: eadd5204.

15. Houghton AM, Rzymkiewicz DM, Ji H, Gregory AD, Egea EE, Metz HE, et al. Neutrophil elastase-mediated degradation of IRS-1 accelerates lung tumor growth. Nat Med. 2010; 16: 219-23.
16. Nywening TM, Belt BA, Cullinan DR, Panni RZ, Han BJ, Sanford DE, et al. Targeting both tumour-associated CXCR2$^+$ neutrophils and CCR2$^+$ macrophages disrupts myeloid recruitment and improves chemotherapeutic responses in pancreatic ductal adenocarcinoma. Gut. 2018; 67: 1112-23.
17. Ame JC, Spenlehauer C, de Murcia G. The PARP superfamily. Bioessays. 2004; 26: 882-93.
18. Luscher B, Ahel I, Altmeyer M, Ashworth A, Bai PT, Chang P, et al. ADP-ribosyltransferases, an update on function and nomenclature. FEBS J. 2022; 289: 7399-410.
19. Pazzaglia S, Pioli C. Multifaceted role of PARP-1 in DNA repair and inflammation: pathological and therapeutic implications in cancer and non-cancer diseases. Cells. 2019; 9: 41.
20. Wang G, Huang X, Li Y, Guo K, Ning P, Zhang Y. PARP-1 inhibitor, DPQ, attenuates LPS-induced acute lung injury through inhibiting NF-γb-mediated inflammatory response. PLoS One. 2013; 8: e79757.
21. Dharwal V, Naura AS. PARP-1 inhibition ameliorates elastase induced lung inflammation and emphysema in mice. Biochem Pharmacol. 2018; 150: 24-34.
22. Raftopoulou S, Valadez-Cosmes P, Mihalic ZN, Schicho R, Kargl J. Tumor-mediated neutrophil polarization and therapeutic implications. Int J Mol Sci. 2022; 23: 3218.
23. Chabanon RM, Muirhead G, Krastev DB, Adam J, Morel D, Garrido M, et al. PARP inhibition enhances tumor cell-intrinsic immunity in ERCC1-deficient non-small cell lung cancer. J Clin Invest. 2019; 129: 1211-28.
24. Wang G, Zhou X, Guo Z, Huang N, Li J, Lv Y, et al. The anti-fibrosis drug Pirfenidone modifies the immunosuppressive tumor microenvironment and prevents the progression of renal cell carcinoma by inhibiting tumor autocrine TGF-β. Cancer Biol Ther. 2022; 23: 150-62.
25. Wang G, Cao L, Liu X, Sieracki NA, Di A, Wen X, et al. Oxidant sensing by TRPM2 inhibits neutrophil migration and mitigates inflammation. Dev Cell. 2016; 38: 453-62.
26. Chen Y, Han L, Qiu X, Wang M, Chen Z, Cai Y, et al. Reassembling of albumin-bound paclitaxel mitigates myelosuppression and improves its antitumoral efficacy via neutrophil-mediated targeting drug delivery. Drug Deliv. 2022; 29: 728-42.
27. Lanczky A, Gyorffy B. Web-based survival analysis tool tailored for medical research (KMplot): Development and implementation. J Med Internet Res. 2021; 23: e27633.
28. Papayannopoulos V. Neutrophil extracellular traps in immunity and disease. Nat Rev Immunol. 2018; 18: 134-47.
29. Cathcart J, Pulkoski-Gross A, Cao J. Targeting matrix metalloproteinases in cancer: bringing new life to old ideas. Genes Dis. 2015; 2: 26-34.
30. Kessenbrock K, Plaks V, Werb Z. Matrix metalloproteinases: regulators of the tumor microenvironment. Cell. 2010; 141: 52-67.
31. Vannitamby A, Seow HJ, Anderson G, Vlahos R, Thompson M, Steinfort D, et al. Tumour-associated neutrophils and loss of epithelial PTEN can promote corticosteroid-insensitive MMP-9 expression in the chronically inflamed lung microenvironment. Thorax. 2017; 72: 1140-3.
32. Lee SJ, Kim CE, Yun MR, Seo KW, Park HM, Yun JW, et al. 4-hydroxynonenal enhances MMP-9 production in murine macrophages 5-lipoxygenase-mediated activation of ERK and p38 MAPK. Toxicol Appl Pharm. 2010; 242: 191-8.
33. Kim CE, Lee SJ, Seo KW, Park HM, Yun JW, Bae JU, et al. Acrolein increases 5-lipoxygenase expression in murine macrophages through activation of ERK pathway. Toxicol Appl Pharm. 2010; 245: 76-82.
34. Tu XK, Yang WZ, Shi SS, Chen CM, Wang CH. 5-lipoxygenase inhibitor Zileuton attenuates ischemic brain damage: involvement of matrix metalloproteinase 9. Neurol Res. 2009; 31: 848-52.
35. Kummer NT, Nowicki TS, Azzi JP, Reyes I, Iacob C, Xie S, et al. Arachidonate 5 lipoxygenase expression in papillary thyroid carcinoma promotes invasion via MMP-9 induction. J Cell Biochem. 2012; 113: 1998-2008.
36. Wu F, Wang L, Zhou C. Lung cancer in china: current and prospect. Curr Opin Oncol. 2021; 33: 40-6.
37. Quail DF, Joyce JA. Microenvironmental regulation of tumor progression and metastasis. Nat Med. 2013; 19: 1423-37.
38. Hanahan D, Weinberg RA. Hallmarks of cancer: the next generation. Cell. 2011; 144: 646-74.
39. Zilionis R, Engblom C, Pfirschke C, Savova V, Zemmour D, Saatcioglu HD, et al. Single-cell transcriptomics of human and mouse lung cancers reveals conserved myeloid populations across individuals and species. Immunity. 2019; 50: 1317-34.e10.
40. Jaillon S, Ponzetta A, Di Mitri D, Santoni A, Bonecchi R, Mantovani A. Neutrophil diversity and plasticity in tumour progression and therapy. Nat Rev Cancer. 2020; 20: 485-503.

Cite this article as: Han L, Chen Y, Huang N, Zhou X, Lv Y, Li H, et al. Cancer-educated neutrophils promote lung cancer progression *via* PARP-1-ALOX5-mediated MMP-9 expression. Cancer Biol Med. 2024; 21: 175-192. doi: 10.20892/j.issn.2095-3941.2023.0248